Nonlinear time series analysis of geomagnetic pulsations

Z. Vörös, J. Verö, J. Kristek

▶ **To cite this version:**

Z. Vörös, J. Verö, J. Kristek. Nonlinear time series analysis of geomagnetic pulsations. Nonlinear Processes in Geophysics, 1994, 1 (2/3), pp.145-155. hal-00301737

HAL Id: hal-00301737
https://hal.science/hal-00301737v1

Submitted on 18 Jun 2008

HAL is a multi-disciplinary open access archive for the deposit and dissemination of scientific research documents, whether they are published or not. The documents may come from teaching and research institutions in France or abroad, or from public or private research centers.

L'archive ouverte pluridisciplinaire **HAL**, est destinée au dépôt et à la diffusion de documents scientifiques de niveau recherche, publiés ou non, émanant des établissements d'enseignement et de recherche français ou étrangers, des laboratoires publics ou privés.

Nonlinear Processes in Geophysics (1994) 1: 145 - 155

Nonlinear Processes in Geophysics
© European Geophysical Society 1994

Nonlinear time series analysis of geomagnetic pulsations

Z. Vörös[1], J. Verö[2] and J. Kristek[3]

[1] Geophysical Institute SAS, 94701 Hurbanovo, Slovakia
[2] Geodetic and Geophysical Research Institute, 9400 Sopron, Hungary
[3] Geophysical Institute SAS, 84228 Bratislava, Slovakia

Received 10 November 1993 - Accepted 26 April 1994 - Communicated by D. Schertzer

Abstract. A detailed nonlinear time series analysis has been made of two daytime geomagnetic pulsation events being recorded at L'Aquila (Italy, $L \approx 1.6$) and Niemegk (Germany, $L \approx 2.3$). Grassberger and Procaccia algorithm has been used to investigate the dimensionality of physical processes. Surrogate data test and self affinity (fractal) test have been used to exclude colored noise with power law spectra. Largest Lyapunov exponents have been estimated using the methods of Wolf et al. The problems of embedding, stability of estimations, spurious correlations and nonlinear noise reduction have also been discussed. The main conclusions of this work, which include some new results on the geomagnetic pulsations, are **(1)** that the April 26, 1991 event, represented by two observatory time series **LAQ1** and **NGK1** is probably due to incoherent waves; no finite correlation dimension was found in this case, and **(2)** that the June 18, 1991 event represented by observatory time series **LAQ2** and **NGK2** , is due to low dimensional nonlinear dynamics, which include deterministic chaos with correlation dimension $D_2(LAQ2) = 2.25 \pm 0.05$ and $D_2(NGK2) = 2.02 \pm 0.03$, and with positive Lyapunov exponents $\lambda_{max}(LAQ2) = 0.055 \pm 0.003$ bits/s and $\lambda_{max}(NGK2) = 0.052 \pm 0.003$ bits/s; the predictability time in both cases is ≈ 13 s.

1 Introduction

The Earth's magnetosphere is a macroscopic open system with a characteristic permanent state that is far from thermal equilibrium. The non-equilibrium state is ensured by the permanent solar wind - magnetosphere interaction.

Bargatze et al. (1985) have used linear prediction filter technique to show that the magnetospheric response to solar wind energy and mass loading is significantly nonlinear. Baker et al. (1990) have attempted to analyse the loading-unloading cycle of magnetospheric response as an output time pattern of a nonlinear, damped harmonic oscillator. A plasma physics analogue model of substorms was proposed by Klimas et al. (1991). A simple model of the magnetotail which incorporates dynamics and thermodynamics and exhibits chaos was proposed by Goertz et al. (1991). The nonlinear models involve only a few degrees of freedom assuming that, the solar wind-magnetosphere system asymptotes to a low dimensional chaotic attractor in its associated phase space.

The first results of nonlinear time series analysis of AE, AL indices (Vassiliadis et al., 1990; Shan et al., 1991; Pavlos et al., 1992) and local field variations (Vörös, 1991), in fact, supported the idea that, on the time scale of magnetospheric substorms (30-50 min), the number of active degrees of freedom is finite (from 3 to 5). Recently, however, the method (Grassberger and Procaccia, 1983) used in (Vassiliadis et al., 1990; Shan et al., 1991; Vörös, 1991) seems to be ambiguous due to the problems connected with correlation dimension (number of degrees of freedom) estimates of colored noise (Osborne and Provenzale, 1989) and due to spurious correlations (Prichard and Price, 1992). Fortunately, it is not difficult to introduce a correction to spurious correlations (Theiler, 1986). It is also possible to set up reliable criteria for the exclusion of pseudo-chaotic dynamics caused by colored noise (Roberts, 1991; Pavlos et al., 1992). In the latter case, however, the situation is not very simple. Fractal dimensionality (self-similarity) has been shown to be characteristic for H-component of the local field variations (random curve) during geomagnetic storms (Vörös, 1990; De Santis and Chiappini, 1992). It is known that colored random noise is possible to interpret in terms of random fractal curves (Osborne and Provenzale, 1989). It has also been shown that colored noise with two components, bicolored noise, shares many properties with AE index data (Takalo et al., 1993). The reason for this similarity is not clear yet.

Correspondence to: Z. Vörös

A possible explanation of these contradictory results is that magnetosphere time series only exhibit low dimensional behaviour during selected time intervals (activity levels ?). In any case, the solar wind - magnetosphere system should be studied in future, as a nonlinear dynamical input - output system (Prichard and Price, 1992). To be more concrete, we note, the solar wind (kinetic energy $\approx 10^4$ GW) - magnetosphere (dissipated energy 200 - 800 GW) coupling has an efficiency of an average $\approx$ 5%. These 5% are provided by several different transfer processes such as reconnection, diffusion, Kelvin-Helmholtz instability, drift entry, etc. For this reason nonlinear input-output analysis requires a broad-range mapping of the physical processes while the underlying data is supplied by surface as well as satellite measurements.

This paper is devoted to the nonlinear time series analysis of two geomagnetic pulsation events. From the pure energetical point of view pulsation activity represents a petty part of the energy inflow to the magnetosphere (1-10 GW). Elucidating better the complex chain of nonlinear interactions between the solar wind and the magnetosphere field-line structures, however, one may contribute to the understanding of the macroscopic nonlinear input-output system. In this paper, as a first step, we address the problem of identification of deterministic chaos as manifested in time series of pulsation events.

2 Geomagnetic pulsations

The origin of geomagnetic pulsations has been clarified in rough outlines in recent years (Southwood, 1974; Hasegawa et al., 1983; Cz. Miletitz et al., 1990; Vellante et al., 1993). Morphologically several types can be distinguished, the most frequent one is the continuous type Pc2-4. Such pulsations occur at mid-latitudes nearly continuously during daytime hours.

The energy of these pulsations is, however, strongly changing on different time scales, beginning with beat structures (with an envelope of a duration of about 10 cycles) to activities lasting several hours. Impulsive events do occur, too. The activity of the Pc2-4 pulsations has been shown to be controlled by interplanetary parameters: amplitudes by the solar wind velocity, energy and by the cone angle (the angle between the Sun-Earth direction and the direction of the interplanetary magnetic field - IMF), the period by the IMF scalar magnitude. An immediate connection with upstream waves in the pre-magnetospheric solar wind was established, too.

In spite of the connection between interplanetary parameters and pulsations, pulsation periods change with geomagnetic latitude or L-value, indicating serious transformation in the magnetosphere. Thus, connection between pulsation parameters and interplanetary ones are valid rather statistically than in particular cases. Nevertheless, events can be distinguished when the magnetospheric influence is stronger (e.g. the period changes with the L-value, the waveform is regular-sinusoidal) and when it is weaker (period constant at different latitudes, less regular waveform, period changes correspond to changes in the IMF magnitude). Magnetospheric signals are attributed to field line/shell resonances, when the period is determined by the resonance period of a geomagnetic field line or of a shell of field lines. Shells of field lines are supposed to be of a thickness of 100 or a few hundreds of km-s at the surface, and sometimes slightly (by about 10 percent) different periods of neighbouring shells are observed simultaneously (beating structure). Even signals of interplanetary origin and of magnetospheric origin are observed at the same time. Thus, pulsations are due to several, simultaneously active sources which have different characteristics. The previous summary is to be supplemented further by waves coming from the tail, by impulsive excitation (e.g. by substorm onsets, nighttime Pi2 pulsations). In such a situation Pc2-4 activities may have quasi-continuous spectra with resonance peaks, and nonlinear time series analysis may contribute to a separation of signals coming (mostly) from one or other source. As the most significant contribution in the Pc2-4 spectrum comes from upstream waves and field line resonances, the investigation of pulsations is to be concentrated on this aspect. The only doubtless identification of these types is due to a comparison of (dynamic) spectra at different latitudes, at the same meridian, or near to it. That is why the events will be studied in the following at the Central European stations: Niemegk (Germany, $L \approx 2.3$) and L'Aquila (Italy, $L \approx 1.6$).

3 Data analysis in the time and the frequency domain

The first step which should be done in conjunction with the nonlinear methods is to look at the power spectrum by using fast Fourier transform. In this way we can recognize periodic, quasiperiodic and aperiodic motions (discrete, singular continuous and continuous spectra, respectively). On this basis, however, one can not discriminate between chaotic processes with a few active degrees of freedom and stochastic or random processes with a practically infinite number of degrees of freedom.

In spite of it, the spectral method still remains a very useful and indispensable procedure. Even in the cases of quasiperiodic or aperiodic motions, large amount of essential information is possible to obtain by careful examination of spectra. We mention several typical examples that we will use in this work: recognition of characteristic frequency (range) could help in the reconstruction of phase space (see later); enhanced activity in some frequency interval (band) gives information about the underlying physical processes (Pi, Pc pulsations, lo-

cal, global events, wave packets, etc); power-law spectra may indicate fractal structure (Osborne and Provenzale, 1989) ; significant distortion or spurious peak emergence in the spectra warns the researcher that the signal is probably overfiltered, etc.

Fourier transforming the power spectra we compute the autocorrelation function, which, for a chaotic signal, tends to zero as the lag time increases.

4 Nonlinear methods

As input data we use scalar time series of two pulsation events. To follow a proper dynamics of geomagnetic pulsations, we suppose that, after transients' dying down, the system under consideration asymptotes with increasing time to a low dimensional attractor in its associated phase space. After the reconstruction of an artificial phase space (Takens, 1981) we estimate the correlation dimension D_2 (Grassberger and Procaccia, 1983), which is roughly equal to the number of active degrees of freedom (sometimes $2D_2 + 1$ coordinates are needed), and compute the largest Lyapunov exponent (Wolf et al., 1985) which characterize the system's extreme sensitivity to initial conditions. We also use several tests and apply criteria to insure the robustness of estimations and to eliminate the possibility of pseudochaotic dynamics .

4.1 Phase space reconstruction

We create a set of m-dimensional state vectors ($\mathbf{X}_i$) from a single scalar time series $X_i = X(t_i)$, $i = 1, \ldots, N$; by using a time delay (τ) as follows (Takens, 1981)

$$\mathbf{X}_i = (X(t_i), X(t_i + \tau), \ldots, X(t_i + (m-1)\tau)) \qquad (1)$$

For finite amounts of noisy data the choice of time delay is crucial. For small values of τ the reconstructed attractor will be squashed along the phase space diagonal. A delay time which is larger than the characteristic recurrence time of the system causes "overfolding", because flows with contrary directions have separations less than the resolution (Buzug and Pfister, 1992). When τ is too large, noise will dominate and dynamical information will be lost. We use several methods to choose a time delay appropriately.

4.1.1 Attractor covering method

Drawing profit from the above knowledge, we have developed an extremely simple method to find a relevant interval for time delay. In m dimensional phase space we cover an attractor by a grid of defined resolution and then compute the ratio of unfilled to filled boxes (Attractor Covering Method - ACM).This ratio is saturated when τ is too large and the phase space reconstruction is dominated by noise.

Figure 1 shows the relative (percentual) ratio of unfilled to filled boxes (the number of both is usually several hundred depending on grid resolution and embedding dimension) computed for known mathematical systems (using the computed "time series" of 1D Henon map, Lorenz and Rossler attractors). For these systems the proper interval for time delay is from 80% to 90% of the saturated (noise dominated) level.

In addition, checking up the spurious effects caused by improper stretching and folding we examine carefully two dimensional phase space portraits for various time delays, each chosen from those $80\% - 90\%$ interval. "Overfolding" looks like a crumpled sheet of paper (Buzug and Pfister, 1992). We use this method for geomagnetic pulsation data.

4.1.2 "ACF" method

We examine the autocorrelation function (ACF) and accept that the 1/e fraction or the first zero of the ACF leads to delay times which ensure that two coordinates become linearly independent (Schuster, 1989).The method fails for systems of higher dimension.

4.1.3 "Pseudocycle" method

Another simple criterion is to take τ in a range of about 25% of the pseudocycle (characteristic time - T_{CH}) and then pragmatically accept the value for which the correlation dimension is unchanged when τ is varied (Buzug and Pfister, 1992).

For low dimensional systems all these methods should approximately yield the same interval for τ.

4.2 Nonlinear noise reduction

It is expected that the time series of geomagnetic pulsation data will necessarily be noisy. For this reason, we decided to clean the data by a noise reduction algorithm (Schreiber, 1993). The effectiveness of the nonlinear noise reduction algorithm (NNR) was tested by using noisy 1D map data, the Mackey-Glass delay differential equation (Schreiber, 1993), data from a Taylor-Coutte experiment (Schreiber and Grassberger, 1991).

The main idea of the NNR technique (Schreiber, 1993) is to replace each measurement (X_i) by the average value of this coordinate over points in a suitably chosen neighbourhood of radius ρ .The neighbourhoods are defined in a reconstructed phase space and k coordinates from past and future are used to construct embedding vectors $\mathbf{X}_i$. Then the coordinate X_i is replaced by its mean value in $\mathbf{U}_i$

$$X_i \rightarrow X_i^{corr} = \frac{1}{|\mathbf{U}_i^{\rho}|} \sum_{\mathbf{U}_i^{\rho}} \mathbf{X}_j \qquad (2)$$

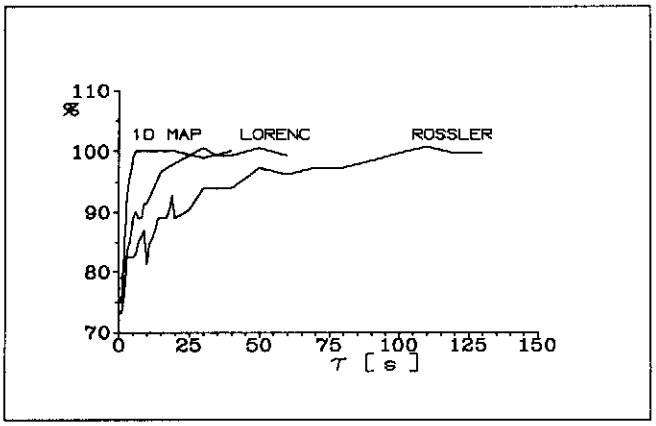

Figure 1. Percentual ratio of unfilled to filled boxes as a function of time delay τ. Embedding dimension is fixed to $m = 4$.

where $\mathbf{U}_i^{\rho}$ is the set of all neighbours for which

$$\| \mathbf{X}_j - \mathbf{X}_i \|_{sup} < \rho$$

In every case it is necessary to examine carefully the effects of the cleaning. To this end we always generate several realizations of cleaned time sequences (symbolically $\{NNR(k,\rho)X_i\}$), and only those parameters (k and ρ) are considered for further computations, for which the correlation dimension estimation leads to the equal values (within error bars). The occasional distortion of the power spectrum due to overfiltering is also examined (an emergence of spurious peaks should yield a spuriously low correlation dimension).

4.3 Correlation dimension

Following the procedure proposed by Grassberger and Procaccia (1983) , a reference phase space point $\mathbf{X}_i$ is chosen and all its distances $|\mathbf{X}_i - \mathbf{X}_j|$ from the N-1 remaining points are computed. For a chaotic attractor a scaling law exists for the number of data points that are within a prescribed distance ε from point $\mathbf{X}_i$

$$\varepsilon^{D_2(m)} \approx \chi \sum_{j=W}^{N} \sum_{i=1}^{N-j} \Theta(\varepsilon - \| \mathbf{X}_i^m - \mathbf{X}_j^m \|) = C_m^{\varepsilon} \qquad (3)$$

and

$$\chi = \frac{2}{(N-W)(N-W+1)}$$

where D_2 is the correlation dimension; N is the number of data points ($N \approx 10^D$ is the minimum number of data points required to reconstruct an attractor properly); Θ is the Heaviside step function; m is the embedding dimension; C_m^{ε} is the correlation sum; Euclidean norm is used. Those points for which $|i-j|\delta t$ ($\delta t = t_{i+1} - t_i$) is less than the autocorrelation time ($\approx W$) are excluded (correction to spurious correlations - Theiler, 1986).

If we subsequently compute $D_2(m)$ in a phase space of increasing dimension m, then for chaotic time series,

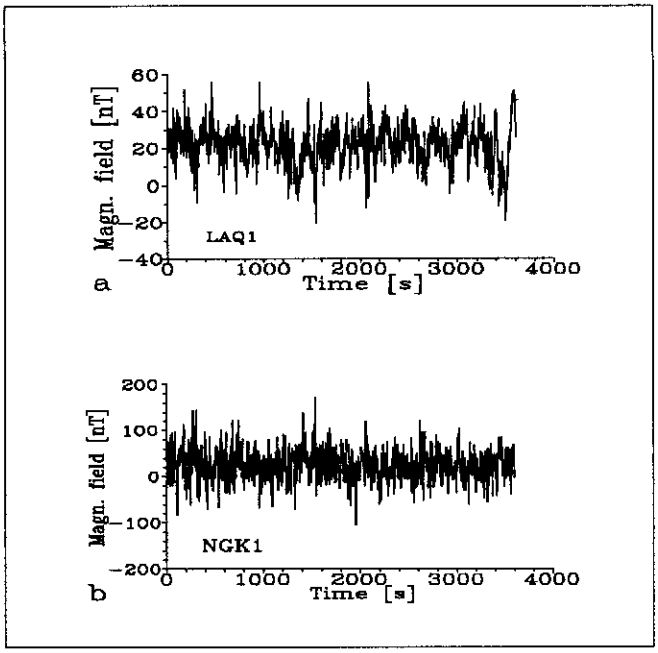

Figure 2. Geomagnetic pulsation time series –event April 26, 1991– with 1s time resolution, registered at a L'Aquila (**LAQ1**); b Niemegk (**NGK1**)

$D_2(m)$ reaches its saturation limit. A convenient way to visualize the dependence of $D_2(m)$ on $ln(\varepsilon)$ is to plot the slope of $\Delta \ln C_m(\varepsilon)/\Delta \ln(\varepsilon)$ versus $\ln(\varepsilon)$. If, for increasing value of m, there is a statistically significant scaling region (with lower and upper limit) where the slope remains constant, then this saturation value of the slope will be considered as the correlation dimension. The robustness of the whole procedure will be tested for several values of time delay .

For the exclusion of pseudochaotic signals (colored noise) the following two criteria are involved, too.

4.3.1 Surrogate data test

Randomizing the phases of the Fourier transform of the original time series and then inverting the transform we create several (≈ 5) realizations of surrogate data with same spectra and ACF as of the original time series. After it we recalculate D_2 for each of the surrogate data. If the results do not significantly differ from those of the original time series, the dimension estimate should not be trusted (Roberts, 1991).

4.3.2 Self-affinity (fractal) test

Self-affinity means that if the time scale is rescaled by a factor η and the signal itself is rescaled by a factor η^{-H} , then the transformed time series has the same statistical properties as the original one. If the signal is self-affine, then (Osborne and Provenzale, 1989)

$$\langle |X(t_i + \eta\delta t) - X(t_i)| \rangle = \eta^H \langle |X(t_i + \delta t) - X(t_i)| \rangle \qquad (4)$$

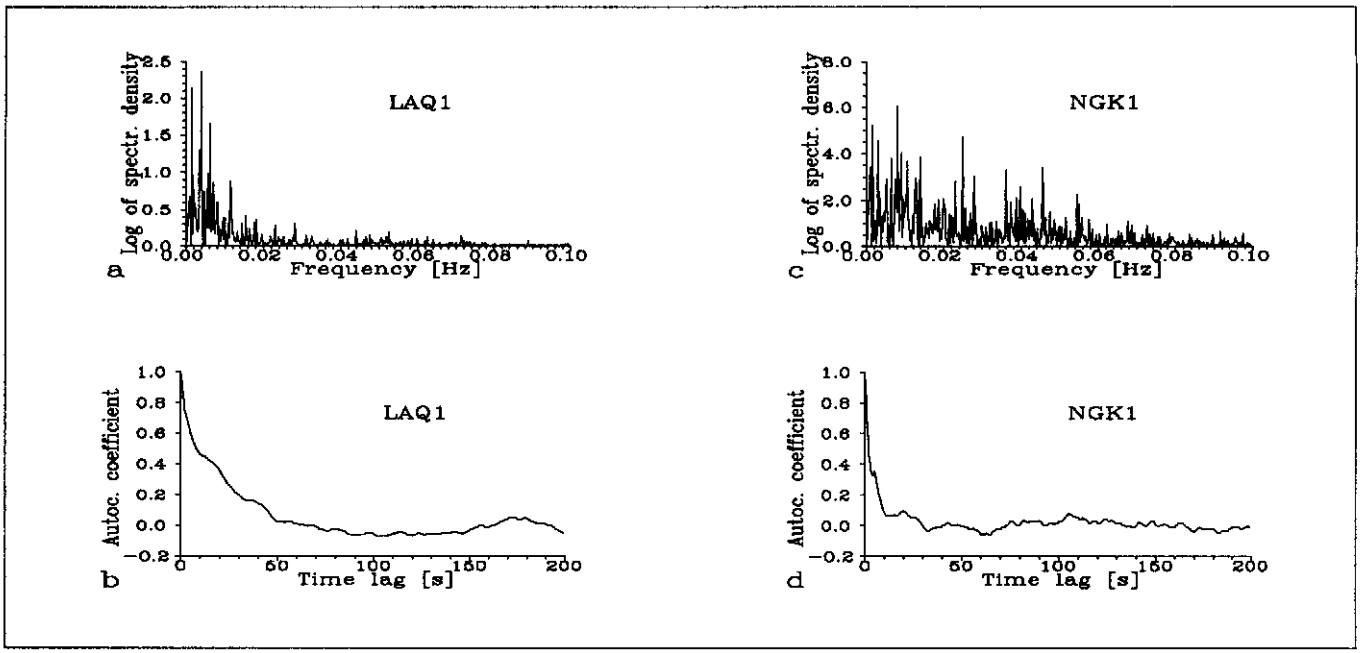

Figure 3. a The power spectrum of the **LAQ1** data; b the autocorrelation function of the **LAQ1** data; c the power spectrum of the **NGK1** data; d the autocorrelation function of the **NGK1** data

where the symbol $\langle\ \rangle$ indicates time average; H is the self-affinity scaling exponent - a slope of the straight line in a log-log plot of $\langle|X(t_i+\eta\delta t)-X(t_i|\rangle$ versus η; η is the scaling factor. A kind of colored noise with power law spectra is self-affine, and in this case the Grassberger and Procaccia (1983) algorithm measures the fractal dimension of a self-affine curve instead of the correlation dimension D_2 which is related to the nonlinear system's dynamics. Therefore, if a time series shares several properties of colored noise (similar spectral exponent, single fractal dimension - straight line in the log-log plot as above), the correlation dimension estimate should not be trusted.

4.4 Largest Lyapunov exponent

In general, the spectrum of Lyapunov exponents, λ_i, may be calculated by linearizing the relevant equations of motion and studying the evolution of small perturbations (Haken, 1983). If $\lambda_i > 0$, $i = 1, 2, \ldots, m$; the motion along trajectories is unstable and small perturbations grow exponentially with time.

In an experimental situation the computation of the whole spectrum of the Lyapunov exponents is quite difficult (Grassberger et al., 1991). An interactive program package written by Wolf et al. (1985) allows us to estimate easily the largest Lyapunov exponent using the relation

$$\lambda_{max} \approx \frac{1}{t_M - t_0} \sum_{i=1}^{M} \log_2 \frac{L'(t_i)}{L(t_{i-1})}; \quad \left[\frac{bits}{s}\right] \tag{5}$$

where $L(t_i)$ denotes the distance which separates two nearby trajectories in the reconstructed phase space; $L(t_0)$ is the distance between two initial points. The initial length will have evolved to length $L'(t_1)$, etc. The total number of replacement steps is M, and the replacement vectors are reorthogonalized from time to time by means of a Gram-Schmidt procedure.

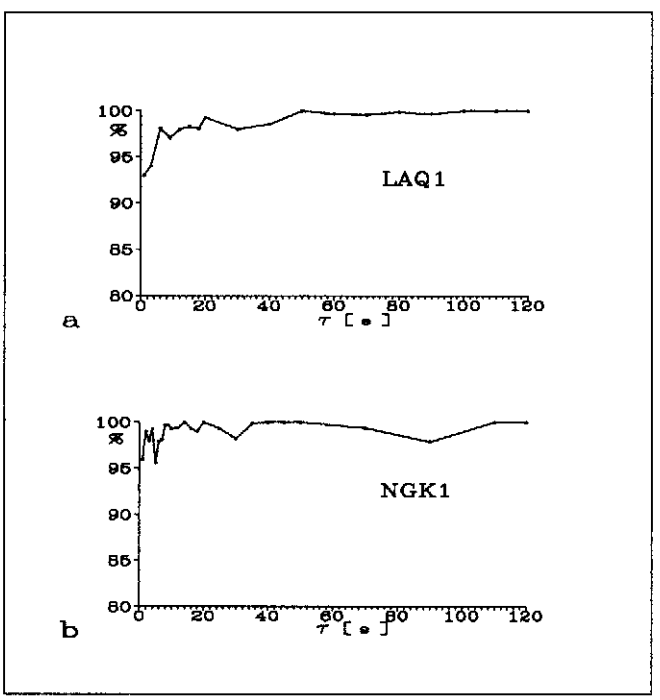

Figure 4. Same plots as in Fig.1 for the a **LAQ1**, b **NGK1** time series.

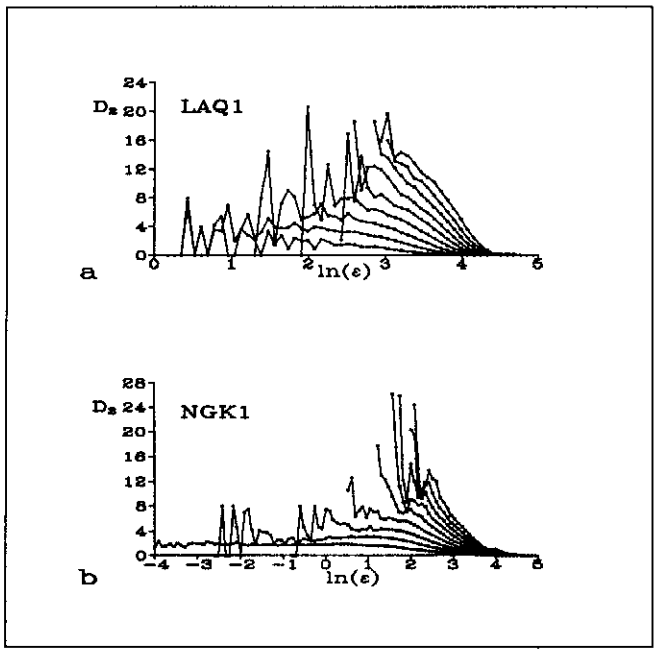

Figure 5. Correlation dimension estimates (D_2) – slopes of $\Delta \ln C_m^\epsilon / \Delta \ln(\epsilon)$ versus $\ln(\epsilon)$ for $m = 2,4,6,8,10,12,14,16,18$ and $\tau = 30$, $k = 10$, $\rho = 30$ a **LAQ1** data, b **NGK1** data

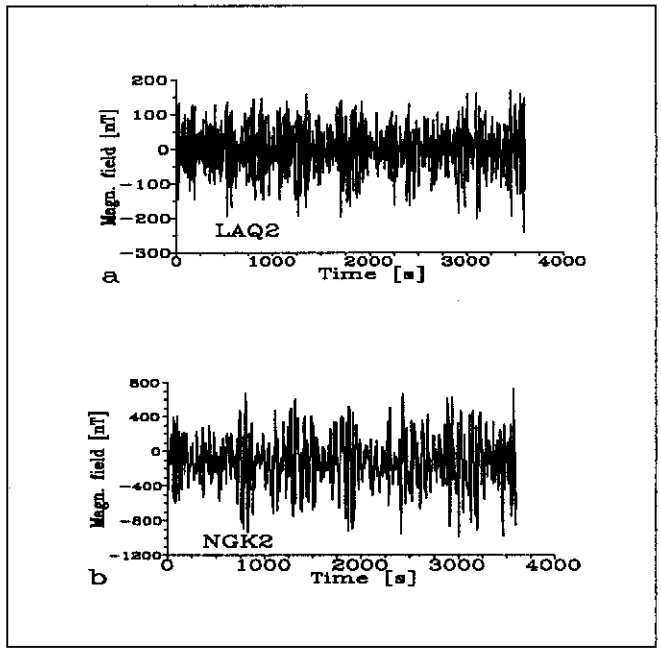

Figure 6. Geomagnetic pulsation time series - event June 18, 1991 - with 1s time resolution; a L'Aquila (**LAQ2**), b Niemegk (**NGK2**)

Supposing that, $\lambda_1 \equiv \lambda_{max} \gg \sum_i \lambda_i, i = 2, \ldots, m$; the predictability or error doubling time may be estimated as

$$T_{PREDICT} \approx \frac{\log_2 2}{\lambda_{max}} \tag{6}$$

We will compute the largest Lyapunov exponent only for pulsation events for which the above procedure proves the existence of deterministic low dimensional dynamics. Again, the results must be stable over changes in all parameters such as time delay, evolution time between replacement steps, maximum and minimum length of replacement vectors allowed, number of data points; unstable estimates should not be trusted (Wolf et al., 1985).

5 Data analysis

We analyse simultaneous observations of two daytime pulsation events recorded at Niemegk (Germany) and L'Aquila (Italy)

. April 26, 1991; 14.00 - 15.00 UT; sampling freq.:$1s^{-1}$; $N = 3600$.

. June 18, 1991; 08.00 - 09.00 UT; sampling freq.:$1s^{-1}$; $N = 3600$.

5.1 Event of April 26,1991

Figure 2a shows the time series of the X component of geomagnetic pulsation as it was recorded at L'Aquila (**LAQ1**). The profile of this time series reveals a stationary process. Figure 2b shows the time series of Y component of the same event, but registered at Niemegk (**NGK1**). The X component of the **NGK1** data is weakly stationary only, this is why instead of it, the more stationary Y component is used.

Figures 3a-d present the power spectral densities (log-scale) and the ACF of the time series **LAQ1** and **NGK1**, respectively. All the spectra shown in this paper is smoothed by using a GEO (Goodman, Enochson, Otnes) window. The power spectra in both cases reveal Pc4 band activity (frequency range $\approx 0.007 - .02Hz$; period range $\approx 50 - 150s$), however, a local Pc3 band activity (frequency range $\approx 0.02 - 0.1Hz$; period range $\approx 10 - 50s$) is present in **NGK1** time series spectrum. If we take the frequency interval from 0.006 to $0.01Hz$ as a prevailing part of the spectra , then the characteristic "period" is about of $\approx 100 - 170s$ and the optimal delay time interval is (pseudocycle method) $\tau = 0.25T_{CH} \approx (25 - 43)s$.

The delay times obtained form the autocorrelation functions (Figs. 3b,d) are ("ACF" method)

. $\tau(LAQ1) \approx (ACF(1/e) - ACF(0))_{LAQ1} \approx (20 - 60)s$

. $\tau(NGK1) \approx (ACF(1/e) - ACF(0))_{NGK1} \approx (4 - 30)s$

On this basis, it seems to be reasonable to choose a time delay from the interval $\tau \in (20 - 30)s$. Using the "ACM" method we have plotted Figs. 4a and b which show no relevant interval ($\approx (80 - 90)\%$ of saturated level) for time delay.

After these preparatory steps, we have computed the correlation dimension for several values of time delay $\tau \in (20, 30)s$; and several realizations of cleaned

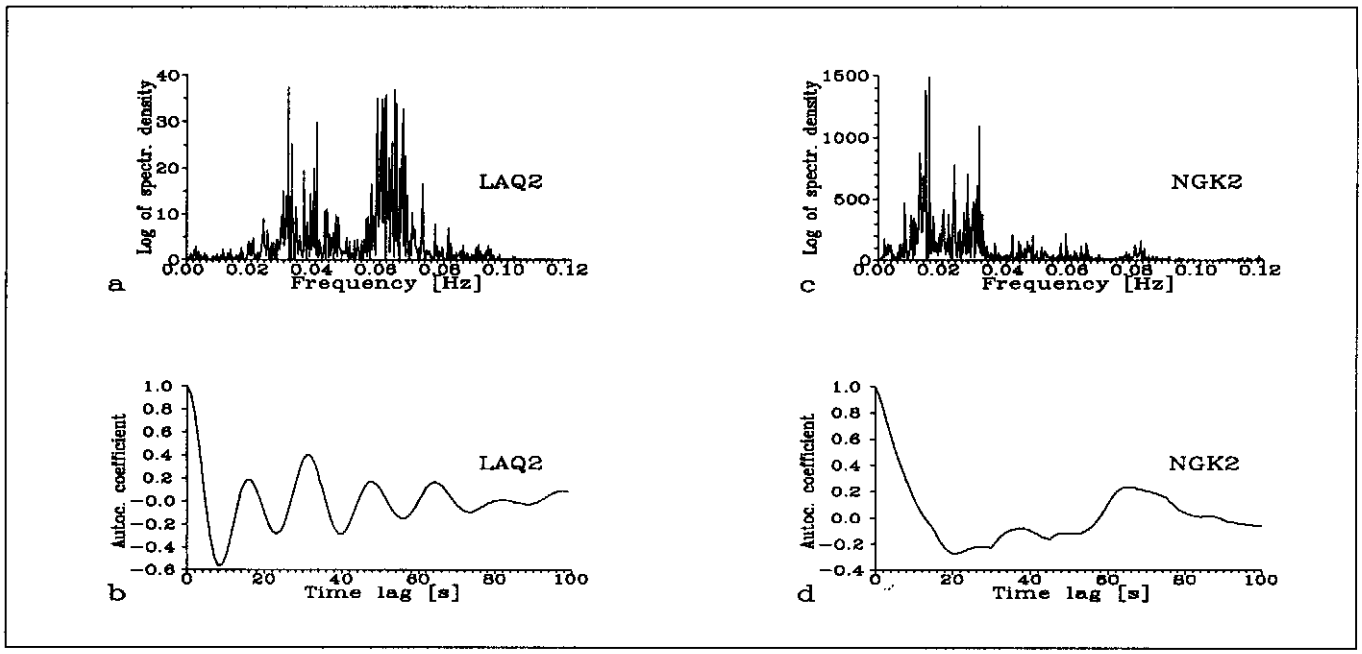

Figure 7. a – d same plots as in Fig.3 for **LAQ2** and **NGK2** time series respectively.

data $\{NNR(k,\rho)LAQ1\}$; $\{NNR(k,\rho)NGK1\}$; $k = 10, 20, 30$ and $\rho = 10, 20, 30, 40, 50$ (in units of the measurements). Independently on parameter values (τ, k, ρ) and observatories (LAQ, NGK) no finite correlation dimension was found. Figures 5a and b show two examples for both time series with parameter values of $\tau = 30, k = 10, \rho = 30$. We have introduced a correction to spurious correlations by choosing $W = 30$ (see Eq.3). The result is in good agreement with the indication of the "ACM" method, namely, that the phase space portraits of both **LAQ1** and **NGK1** data are dominated by noise for any value of τ. An additive noise is possible to remove by using the NNR technique of the data cleaning, however, in our case the correlation dimension for both cleaned time series was not altered significantly. The pulsation event under consideration is not finite dimensional, therefore we do not compute the largest Lyapunov exponent and do not make further tests or examinations.

5.2 Event of June 18, 1991

Figures 6a and b show the stationary time series of the X components of the event registered at L'Aquila (**LAQ2**) and Niemegk (**NGK2**). Figures 7a - d present the power spectral densities and the ACF for both time series. The global behaviour of the pulsation activity was similar at the two stations (the peak about $0.032Hz - 31s - Pc3$ band), however, local spectral pecularities clearly emerged in the experimental observations. Significant peaks emerge at $0.056 - 0.074Hz$ $(13 - 18s - Pc3$ band; **LAQ2**), and at $0.008 - 0.02Hz (50 - 125s - Pc4$ band; **NGK2**).

If we take a common peak at $\approx 0.032Hz$ as a characteristic frequency for the event, then the pseudocycle method gives a time delay of $\tau \approx 8s$. The delay time intervals obtained from the autocorrelation functions (Figs. 7b,d) are ("ACF" method)

- $\tau(LAQ2) \approx (ACF(1/e) - ACF(0))_{LAQ2} \approx (3 - 5)s$
- $\tau(NGK2) \approx (ACF(1/e) - ACF(0))_{NGK2} \approx (6 - 12)s$

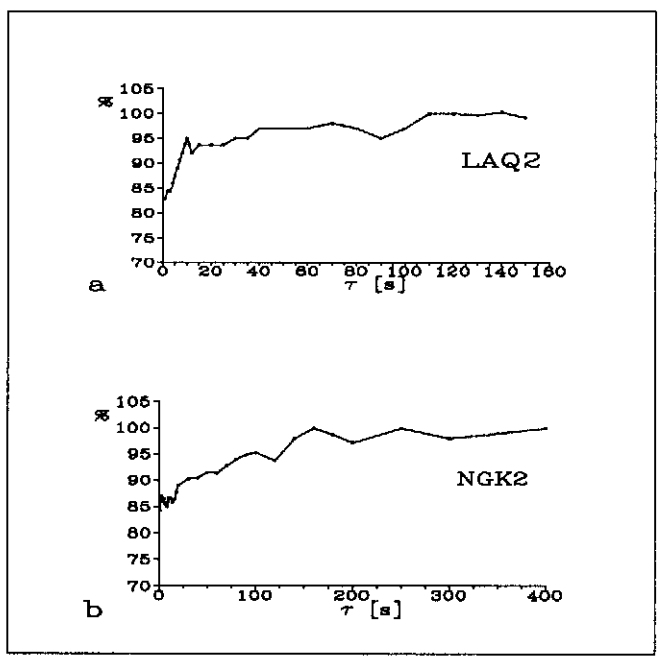

Figure 8. Same plots as in Fig.1 for a **LAQ2** , b **NGK2** data

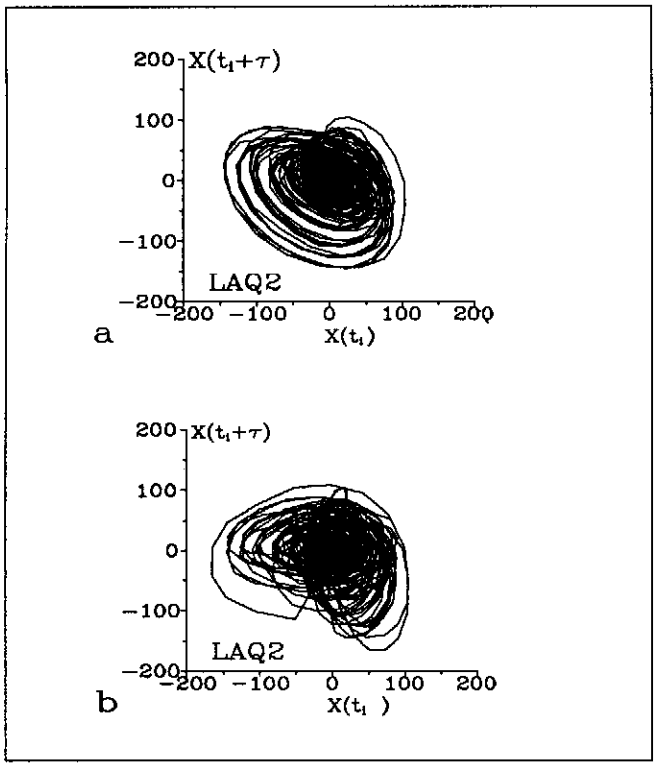

Figure 9. Two dimensional phase space portraits of cleaned **LAQ2** data ($k = 8, \rho = 60$) with a $\tau = 5s$, b $\tau = 12s$ - a spurious stretching and folding effect

The outputs of the "ACF" method are shown in Figs. 8a and b. For **LAQ2** (Fig.8a) the relevant values of time delay are from the interval $\tau \in (1,7)s$, and for **NGK2** (Fig. 8b) from the interval $\tau \in (1,20)s$. For the smallest values of τ the phase portraits are squashed along the phase space diagonal. Due to this insensitiveness of the "ACF" method we use (as above) several methods to choose an appropriate interval for time delay.

Figures 9a and b show two dimensional phase space portraits of cleaned **LAQ2** data ($NNR(k = 8, \rho = 60)$) for two values of time delay chosen within ($\tau = 5$ s - Fig.9a) and without ($\tau = 12$ s - Fig 9b) the proper interval for **LAQ2**. Figure 9b present a clear over-folding (spurious stretching and folding) effect. Taking into account the above indications, we have computed the correlation dimension for the values of time delay from the following intervals: $\tau(LAQ2) \in (1,7)s$ and $\tau(NGK2) \in (4,20)s$. Several realizations of cleaned data were also used: $\{NNR(k,\rho)LAQ2\}$ with $k = 8, 10, 20$ and $\rho = 40, 60, 80$ and $\{NNR(k,\rho)NGK2\}$ with $k = 15, 20, 30$ and $\rho = 40, 60, 80$. A correction to spurious correlations was choosen to be equal to the ACF(0).

Figures 10a and b show examples of the saturation of correlation dimension estimates. As it can be seen the scaling region is broader in the case of **LAQ2** (Fig.10a) $ln(\varepsilon) \approx (-2) - 5$; while for **NGK2** (Fig. 10b) it is $ln(\varepsilon) \approx 4.5 - 6.8$.

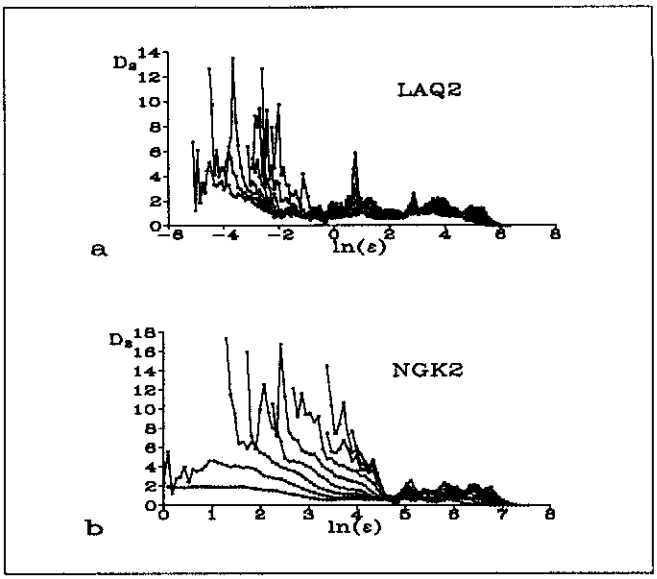

Figure 10. Correlation dimension estimates as in Fig.5 for a **LAQ2** ($\tau = 5, k = 8, \rho = 20$) and b **NGK2** ($\tau = 12, k = 20, \rho = 400$)

Figures 11a (**LAQ2**) and 11b (**NGK2**) show the stability of the correlation dimension computation over the choosen ranges of time delay τ . In accordance with previous expectations, the value of D_2 is underestimated for smaller values of τ , in both cases. The saturated values are $D_2(LAQ2) = 2.25 \pm 0.05$ and $D_2(NGK2) = 2.02 \pm 0.03$. Using only the first 1000 points of **LAQ2** or **NGK2** data the dimension may be estimated by an error of $\approx 20\%$.

To exclude a pseudochaotic signal as a possible stochastic source of low correlation dimension estimate, we have tested our results (see Sect.4.3).

Figures 12a (**LAQ2**) and 12b (**NGK2**) present two examples (from 2×5 realizations) of the surrogate data test. It can be seen that the results are significantly different (no saturation) than those of the original time series.

The results of the fractal test are shown in Fig. 13a (**LAQ2**) and 13b (**NGK2**). No straight lines are present in the log-log plots, therefore the data are not self-affine.

On this basis we can make a statement: the event represented by two observatory time series (**LAQ2** and **NGK2**) is not similar to a colored noise with power law spectra.

The next step is the computation of largest Lyapunov exponents from experimental data.

Figure 14a presents estimates of the λ_{max} for the **LAQ2** time series as a function of time and evolution time. Figure 14b shows the same, but for **NGK2** data. Stability of Lyapunov exponent estimation over changes in time delay, evolution time, maximum and minimum cutoff was examined, too. The estimates stabilize at positive values

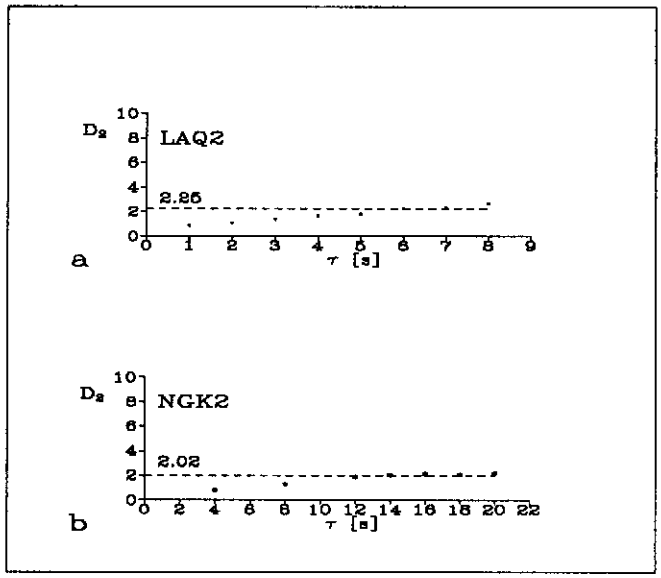

Figure 11. Correlation dimension versus time delay a **LAQ2**, b **NGK2**

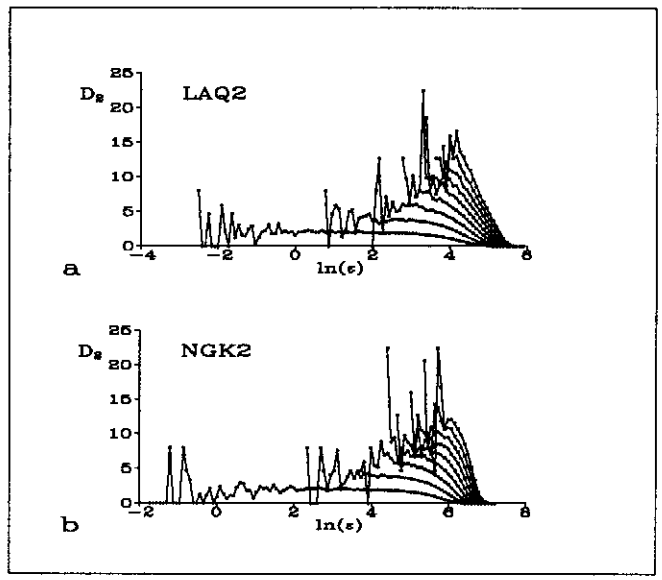

Figure 12. Surrogate data test a **LAQ2**, b **NGK2**

$\lambda_{max}(LAQ2) = 0.055 \pm 0.003 bits/s$

and

$\lambda_{max}(NGK2) = 0.052 \pm 0.003 bits/s$

The predictability times or error doubling times (Eq.6) are

$T_{PREDICT}(LAQ2) \approx T_{PREDICT}(NGK2) \approx 13s$

It is also important to test the temporal convergence of λ_{max} as a function of the number of data points. The obtained convergence rates indicate that it is sufficient to have $\approx$ 2000 data points in the case of **LAQ2** data and $\approx$ 2500 data points in the case of **NGK2** data to estimate a saturated value of λ_{max}.

6 Summary and discussion

In this paper we applied a nonlinear time series analysis to geomagnetic pulsation data.

In the case of the April 26, 1991 event, no finite correlation dimensions were found for **LAQ1** and **NGK1** time series. Therefore, our conclusion is that this event is probably due to incoherent waves (stochastic process). We have not computed the largest Lyapunov exponent for this event.

It has been shown (Anderson , 1993) that incoherent waves comprise a significant fraction of observed fluctuations, and are associated with increased geomagnetic activity for both daytime and nighttime events. In fact, the event represented by **LAQ1** and **NGK1** time series appeared during a geomagnetic storm (sudden storm commencement on April 24). The average Dst index was decreased significantly, too (Solar Geophysical Data, 1991, 1992). The mechanisms for incoherent waves have not been determined, however, it is likely that they are related to magnetic reconfiguration associated with substorms or/and to nonlinear generation and evolution of broadband instabilities.

Finite correlation dimensions were obtained in the case of June 18, 1991 event; $D_2(LAQ2) = 2.25 \pm 0.05$ and $D_2(NGK2) = 2.02 \pm 0.03$. The estimates have been shown to be stabilized over a reasonable range of values of time delay. Fractal and surrogate data tests have shown that the low correlation dimensions do not arise from colored noise with power law spectra, although the debate about stochastic or deterministic nature of geomagnetic pulsations with low correlation dimension should not be entirely closed.

The largest Lyapunov exponents are equal at the two stations within the error bars; $\lambda_{max}(LAQ2) = 0.055 \pm 0.003\ bits/s$ and $\lambda_{max}(NGK2) = 0.052 \pm 0.003\ bits/s$. It has also been shown that the estimates are stable over changes in parameters such as time delay, evolution time, maximum and minimum length of replacement vector allowed, moreover, that the **LAQ2** and **NGK2** time series contain a sufficient number of data points to insure a convergence of λ_{max}.

The above results indicate that an appropriate low dimensional nonlinear model may explain significant aspects of the analysed $Pc3-4$ pulsation event, however, due to the sensitive dependence on initial conditions predictions will be affected by error's exponential growth. The characteristic predictability time is $\approx 13s$.
It is intriguing that the second event (**LAQ2**, **NGK2**), which also appeared during a geomagnetic storm (sudden storm commencement on June 17 - Solar Geophysical Data 1991), shows a deterministically chaotic behaviour while the first event (**LAQ1**, **NGK1**) does

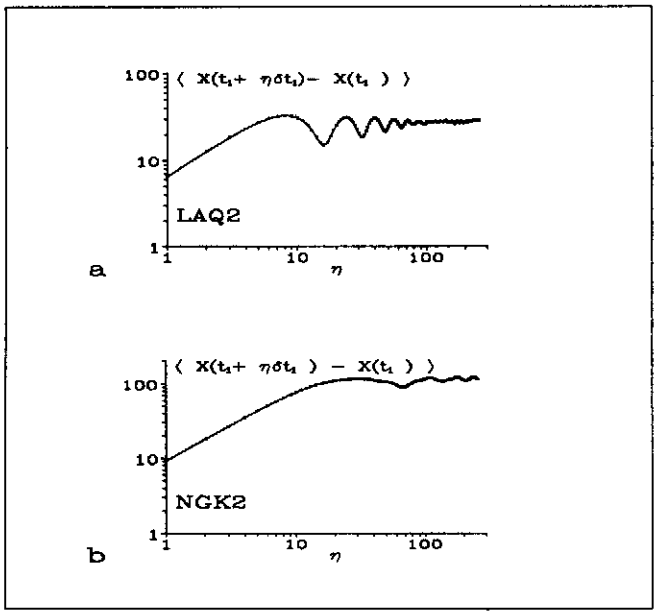

Figure 13. Self-affinity (fractal) test a **LAQ2**, b **NGK2**

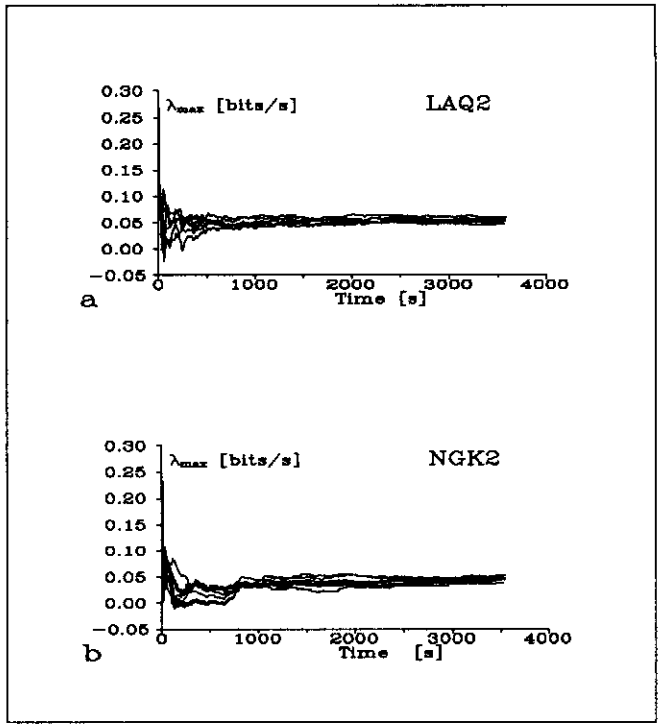

Figure 14. The largest Lyapunov exponent λ_{max} as a function of time and evolution time a **LAQ2**, evolution time = 4, 6, 8, 12, 15, 20, 25 s; b **NGK2**, evolution time = 2, 4, 6, 8, 10, 12, 15, 20 s.

not. A possible explanation of these results is that emergence of coherent low-dimensional pulsations is related to the nonlinear evolution (competition) of coupled macroscopic modes near criticality. In such case of self-organization, the state of a nonlinear high dimensional system, close to an instability point (linear stability loss) , may be described by few degrees of freedom only whose collective motions, depending on control parameters, give rise to macroscopic coherent structures (Haken, 1983; Klimas et al., 1991) . Consequently, incoherent waves emerge when self-organization does not take place. A similar reasoning was proposed for the explanation of chaotic appearance of substorms (Vörös, 1991; Klimas et al., 1991). At this stage, however, we can not decide if salient features of chaotic characteristics of the magnetosphere plasmas (coherent waves, substorms, etc.) could be explained by common model. Moreover, it is almost certainly impossible to obtain the exact values of dimensions and Lyapunov exponents with data obtained from large, essentially uncontrolled magnetosphere - ionosphere open and dissipative system. However, approximate estimates of dimensions and characteristic predictability times may serve as useful empirical measures complementing linear time series analysis results.

Finally we note that much more work is needed to prove the general usefulness of the concepts of deterministic chaos for coherent pulsation activity analysis. That knowledge would be especially important from the point of view of more complex understanding of the solar wind-magnetosphere , nonlinear input-output system.

Acknowledgements. The authors are indebted to dr. Best for the Niemegk, and to dr. Vellante for the L'Aquila records. Reading of the manuscript by dr.D. Watts (Cambridge) is gratefully acknowledged.Work in Hungary was supported by a state grant, OTKA No.1171.

References

Anderson, B. J., Statistical studies of Pc 3-5 pulsations and their relevance for possible source mechanisms of ULF waves *Ann.Geophysicae, 11*, 128–143, 1993.

Baker,D. N., Klimas, A. J., McPherron, R. L., and Büchner, J., The evolution from weak to strong geomagnetic activity, *Geophys.Res.Lett., 17*, 41–44, 1990.

Bargatze, L. F., Baker, D. N., McPherron, R. L., and Hones, E. W. Jr., Magnetospheric impulse response for many levels of geomagnetic activity, *J.Geophys.Res., 90*, 6387–6395, 1985.

Buzug, Th., and Pfister, G., Optimal delay time and embedding dimension for delay time coordinates by analysis of the global static and local dynamical behavior of strange attractors, *Phys.Rev.A, 45*, 7073–7084, 1992.

Cz. Miletitz, J., Verő, J., Ivanova, P., Best, A., and Kivinen, M., Pulsation periods at mid-latitudes –a seven-station study, *Planet.Space Sci., 38*, 85–95, 1990.

De Santis, A., and Chiappini, M., Automatic K scaling by means of fractal and harmonic analysis, *Ann.Geophysicae, 10*, 597–602, 1992

Goertz, C. K., Smith, R. A., and Shan, L. H., Chaos in the plasma sheet, *Geophys.Res.Lett., 18*, 1639–1642, 1991.

Grassberger, P., and Procaccia, I., Characterization of strange attractors, *Phys.Rev.Lett., 50*, 346–349, 1983.

Grassberger, P., Schreiber, T., and Schaffrath, C., Nonlinear time sequence analysis, *Int.J.Bifurcat.Chaos, 1*, 521–547, 1991

Haken, H., *Advanced synergetics*, Springer Verlag, 1983

Hasegawa, A., Tsui, K. H., and Assis, A. S., A theory of long-period magnetic pulsations, 3. Local field oscillations,

Geophys.Res.Lett., *10*, 765–767, 1983.

Klimas, A. J., Baker, D. N., Roberts, D. A., Fairfield, D. H., and Büchner, J., A nonlinear dynamic analogue model of substorms, In. *Magnetospheric substorms*, Eds. Kan, J. R., Potemra, T. A., Kokubun, S., and Iijima,T., *64*, 449–459, American Geophysical Union, 1991.

Osborne, A. R., and Provenzale, A., Finite correlation dimension for stochastic systems with power-law spectra, *Physica D*, *35*, 357–381, 1989.

Pavlos, G. P., Kyriakou, G.A., Rigas, A. G., Liatsis, P. I., Trochoutsos, P.C., and Tsonis, A. A., Evidence for strange attractor structures in space plasmas, *Ann. Geophysicae*, *10*, 309–322, 1992.

Prichard, D., and Price, C. P., Spurious dimension estimates from time series of geomagnetic indices, *Geophys.Res.Lett.*, *19*, 1623–1629, 1992.

Roberts, D. A., Is there a strange attractor in the magnetosphere?, *J.Geophys.Res.*, *96*, 16031–16046, 1991.

Schreiber, T., Extremely simple nonlinear noise reduction method, *Phys. Rev. E*, *47*, 2401–2404, 1993.

Schreiber, T., and Grassberger, P., A simple noise reduction method for real data, *Phys. Lett. A.*, *160*, 411–418, 1991.

Schuster, H. G., *Deterministic chaos*, VCH Verlagsgesellschaft, Weinheim, 1989.

Shan , L. H., Hansen, P., Goertz, C. K., and Smith, K. A., Chaotic appearance of the AE index, *Geophys. Res. Lett.*, *18*, 147–150, 1991.

Southwood. D. J., Some features of field line resonance in the magnetosphere, *Planet. Space Sci*, *22*, 483–491, 1974.

Takalo, J., Timonen, J., and Koskinen, H., Properties of AE data and bicolored noise,*University of Jyväskylä prepr.*, *12*, 1993.

Takens, F., Detecting strange attractors in turbulence, In. *Lecture notes in mathematics*, Eds. Rand, D. A., and Young, L. S.,*898*, 366–381, Springer Verlag, 1981.

Theiler, J., Spurious dimension from correlation algorithms applied to limited time series data, *Phys. Rev. A*, *34*, 2427, 1986.

Vassiliadis, D. V., Sharma, A. S., Eastman, T. E., and Papadopoulos, K., Low-dimensional chaos in magnetospheric activity from AE time series, *Geophys. Res. Lett*, *17*, 841–844, 1990.

Vellante, M., Villante, V., Core, R., Best, A., Lenners, D., and Pilipenko, V. A., Simultaneous geomagnetic pulsation observations at two latitudes : resonant mode characteristics, *Ann. Geophysicae*, *11*, 734–741, 1993.

Vörös, Z., Fractal analysis applied to some geomagnetic storms observed at the Hurbanovo geomagnetic observatory, *Ann. Geophysicae*, *8*, 191–194, 1990.

Vörös, Z., Synergetic approach to substorm phenomenon, In. *Magnetospheric substorms*, Eds. Kan, J. R., Potemra, T. A., Kokubun, S., and Iijima, T., *64*, 461–467, American Geophysical Union, 1991.

Wolf, A., Swift, J.B., Swinney, H.L., and Vastano, J., Determining Lyapunov exponents from a time series, *Physica D*, *16*, 285–317, 1985.